Defining Petrophysical Properties of Ultramafic and Mafic Rocks In Terms of Alteration

Cameron Adams *
Centre for Exploration Targeting
School of Earth Sciences
University of Western Australia
35 Stirling Highway, Crawley
Western Australia, 6009
cameron.adams@reasearch.uwa.edu.au

Michael Dentith
Centre for Exploration Targeting
School of Earth Sciences
University of Western Australia
35 Stirling Highway, Crawley
Western Australia, 6009
michael.dentith@uwa.edu.au

SUMMARY

The effects of talc-carbonate alteration and serpentinisation on the physical properties of ultramafic rocks are regularly presented but often as incomplete datasets, and are subsequently poorly understood. The development of integrated and more robust physical property databases is important. Consequently, two Western Australian greenstone terranes have been studied. Data from ~2,000 samples taken from the Plutonic-Marymia Greenstone Belt and the Eastern Gold Fields are presented. New p-wave velocity, magnetic susceptibility, density, apparent porosity, and natural remanent magnetisation data are examined.

An integrated approach of placing empirical petrophysical data within a rigorous mineralogical and petrological framework has been undertaken. The use of Short Wave Infrared (SWIR) spectral data is investigated. SWIR data are shown to be useful for the identification and quantification of talc-carbonate mineralogy of ultramafic rocks. Similarly the identification of variable Mg-Fe chlorite is also beneficial. Petrophysical data are shown to correlate well when compared with talc-carbonate and chlorite spectral mineral data and abundances. Serpentine group mineralogy can be identified, however olivine, quartz and pyroxene minerals are unable to be resolved due poor absorption features in the SWIR. Serpentine mineral species, i.e. lizardite, antigorite, and chrysotile, are also unable to be resolved due to narrowness of wavelength absorption features. It also important to recognise that reported mineral abundances are typically normalised to SWIR active minerals.

Anomalous values of reliable but limited spectrally classified serpentine data have shown two populations of serpentinised rocks within acoustic impedance plots. In particular, one population presents a high p-wave velocity, i.e. 6500-7000m/s, and ubiquitously low density and high magnetic susceptibility. These data suggest the presence of antigorite and or silicification. Consequently, although SWIR classified data have been shown to be appropriate to use for interpreting variable degrees of talc-carbonate alteration, an interpretation of serpentinised rocks should be treated with caution. Furthermore, it is recognised that the uncertainty of SWIR mineral abundance data should be evaluated where SWIR active minerals present overlapping wavelength features.

Key words: Petrophysics; ultramafic; mafic; Plutonic Well Greenstone Belt; Eastern Gold Fields; alteration; porosity; spectral

INTRODUCTION

It is common practice to categorise rock physical property data solely by lithotype. This has led to the development of wide distributions in range within localised studies and global petrophysical databases. Consequently, an uncertain relationship between reliable rock physical properties and geology is ever present. The characterisation of rock physical property data by alteration may mitigate this uncertainty. The use of mineralogical scanners, e.g. spectral, and portable whole-rock geochemical analysers, e.g. portable x-ray fluorescence (pXRF), are able to put petrophysical data in a correct mineralogical context while reducing the subjectivity of the interpretation of type and variable degree of alteration which are often interpreted by an individual geologist.

New data from eight diamond drill cores are presented. The study includes measurements made on four Department of Mines and Petroleum Kalgoorlie Core Library maintained, and publically accessible, diamond drill cores sourced from the Eastern Gold Fields (GUD174, GUD175, KD8, KD330). Remaining studies have been made on diamond drill core from the Plutonic Gold Mine, Western Australia.

METHOD AND RESULTS

Methods:

Portable instruments were used throughout this study. A handheld Acoustic Control Systems UK1401 ultrasonic tester, and a handheld magnetic susceptibility meter were employed at 2m intervals on each drill core. Physical samples were acquired at 5m intervals and density properties determined at the University of Western Australia Petrophysical Laboratory via Archimedes' principle (Emerson, 1990; Lipton & Horton, 2014). Magnetic susceptibility and sonic measurements were also made on these samples. Natural remanent magnetisation measurements are ongoing (Adams & Dentith, 2017) and are being made using a MagneticEarth Qmeter magnetisation meter. 158 samples have presented a reliably measurable magnetic moment, thereby allowing remanent and induced magnetisation intensities to be calculated. Two laboratory-determined test standards (MagneticEarth, 2015) permitted checks of satisfactory reproducibility of magnetic susceptibility and remanent magnetisation intensity. Instrument accuracy was determined to be better than 9% and 5%, respectively.

Mineralogical data are classified by infrared spectral data using an ASDinc. TerraSpec 4 Hi-Res spectrometer. As the contact probe spot size is 10mm, spatially averaged data are deemed to better represent sample heterogeneity, and are therefore more appropriate to compare with bulk physical properties. Subsequently, 6 spectral measurements were made on spatially unique areas of ~550 selected physical samples and averaged for each sample.

The use of spectral data provides a means from which to better classify physical property data. Carbonate, serpentine, amphibole and chlorite minerals are principal mineral constituents and are of interest to understanding of talc-carbonate alteration and serpentinisation of ultramafic and mafic rocks. These minerals have identifiable absorption features within the SWIR spectrum (Hauff, 1983) and are able to be measured by a TerraSpec 4 Hi-Res spectrometer and identified by The Spectral Geologist™ (TSG8) spectral un-mixing software. Furthermore, the lateral shifts in wavelength features readily allow the sub-classification of the iron and magnesium content of some mineral species (e.g. chlorites, amphiboles, carbonates).

Porosity data of altered mafic and ultramafic rocks are often not collected, largely due to the crystalline nature of metamorphosed rocks and ensuing negligible values. However, small variations in porosity and micro-mineral fractures may provide a means from which to study the effects hydration, carbonatisation, or silicification. Porosity data may be at least as important as alteration when considering the variability of rock physical properties (Dentith et al., 2017). Apparent porosity data have been measured (Emerson, 1990) and are presented.

Results:

Figures 1-3 show that the comparison of individual physical property measurements with geologist lithological logs is of limited benefit. Henkel-bivariate plots (Henkel, 1994) have been shown to be useful when discriminating ultramafic and mafic rocks (Adams & Dentith, 2016). Multi-petrophysical plots of p-wave velocity and magnetic susceptibility (Figure 4) and mass susceptibility (Figure 5) are able to distinguish most ultramafic rocks from mafic rocks. An acoustic impedance plot shows that alone seismic data are unable to clearly distinguish most mafic and ultramafic rocks (Figure 6). In general, wide ranges of lithotype-classified physical property values are observed, and are particularly noticeable for rocks logged as ultramafic talc chlorites, komatiites and serpentinites (Figures 4-6). Wide-ranging physical property values are inherent for rocks ambiguously classified as ‘undifferentiated’. Here, ‘undifferentiated’ rocks are shown to range by up to 4000m/s Vp; 100 SI x 10^{-3} magnetic susceptibility; ~0.15g/cm^3 density.

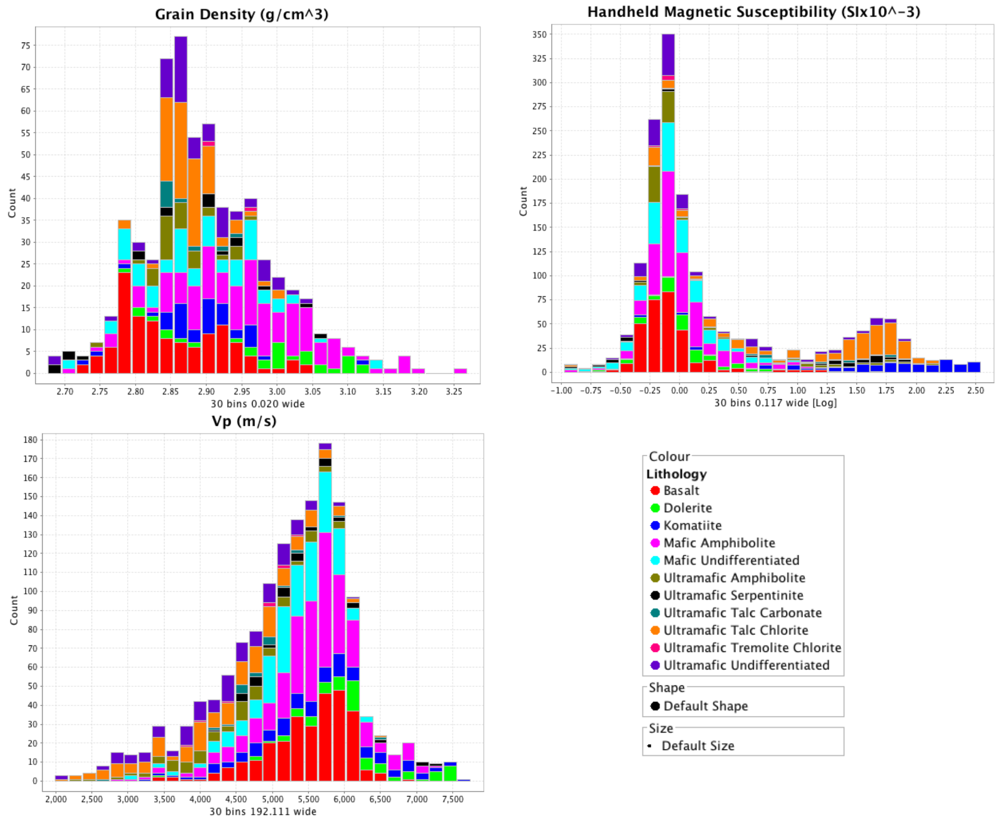

Figures 1-3 (top-left, clockwise): Frequency histograms of physical properties (grain density, magnetic susceptibility, and p-wave velocity, respectively) of studied ultramafic and mafic rocks coloured according to geologist lithological logs. Magnetic susceptibility is in log scale.

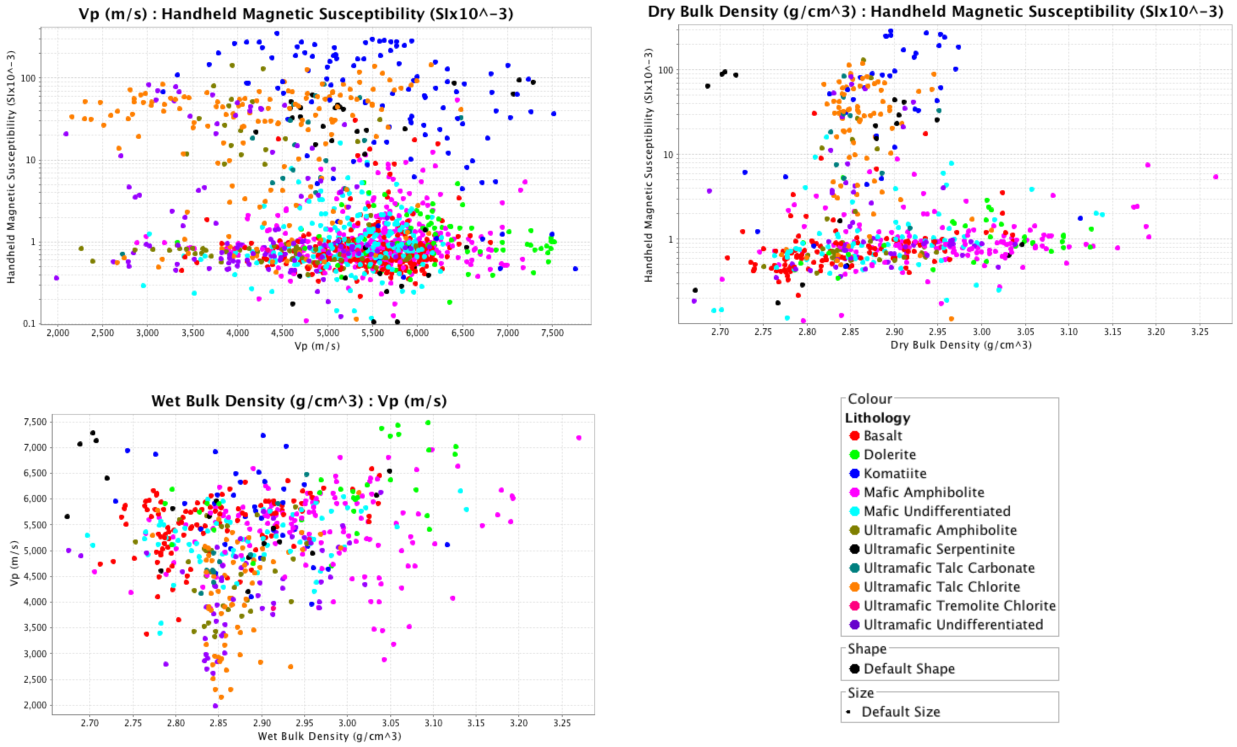

Figures 4-6 (top-left, clockwise): Bivariate physical property plots of p-wave velocity vs magnetic susceptibility; dry bulk density vs magnetic susceptibility (i.e. mass susceptibility); and wet bulk density vs p-wave velocity (i.e. acoustic impedance). Data are from studied ultramafic and mafic rocks, and coloured according to geologist lithological logs. Magnetic susceptibility is in log scale.

As shown in Figures 7 & 8, most ultramafic talc-Mg-rich-chlorite samples (Figures 9-21) have a Q<1 indicating that induced magnetisation is dominant. Prograde talc-carbonate alteration along with a subtle increase in porosity may permit a reduction of magnetic grain size, thereby altering larger multi-domain magnetic grains to single-domain magnetic grains. The magnetism of these fine single-domain grains readily aligns with an applied magnetic field, and is isotropic (Adams & Dentith, 2018). Although not presented, preliminary whole-rock geochemical studies show that some of the ultramafic samples with low porosity are more silica rich. Silica may help to partially preserve magnetic grains from the destruction by talc-carbonate alteration, hence explaining relatively high p-wave velocity, magnetic susceptibility, and a Q>1.

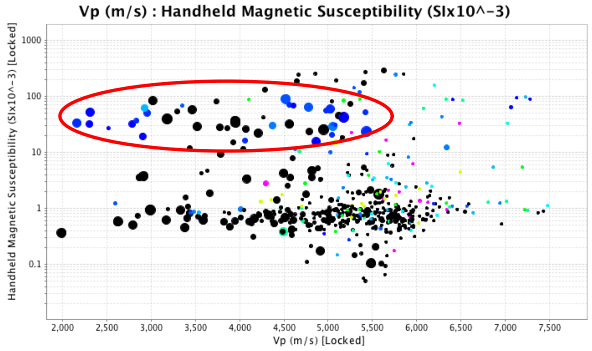

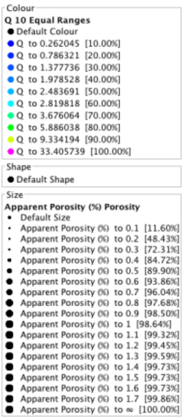

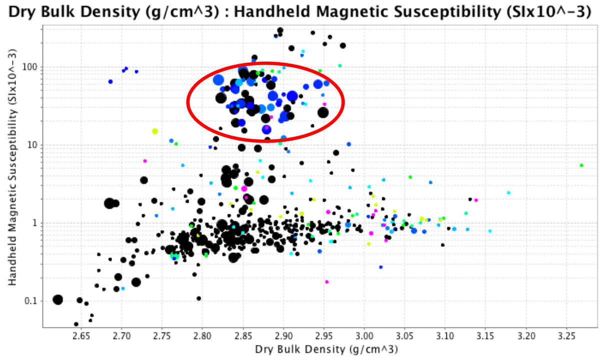

Figures 7 & 8 (top-left and left): Bivariate physical property plots of p-wave velocity vs magnetic and dry bulk density vs magnetic susceptibility, i.e. mass susceptibility. Data are from studied ultramafic and mafic rocks, and coloured according to Q. Data points are sized according to increasing apparent porosity. Magnetic susceptibility is in log scale. Red ellipses show a population of primarily talc-Mg-rich-chlorite samples.

SWIR spectroscopy is able to classify most dominant mineralogy in altered ultramafic and mafic rocks, and is thereby capable of removing the subjectivity, and often misinterpretation, of a logging geologist. Lateral variations in wavelength absorption features allow the sub-classification of chlorite, carbonate, and amphibole mineral species via magnesium and iron content. This is important, as ultramafic rocks are typically magnesium-rich and the difference in dominant mineral species is often difficult to visually determine. Visual interpretation often leads to ultramafic rocks being classified incorrectly as mafic or 'undifferentiated'. The misinterpretation of lithology as well as alteration mineralogy has led to a large range of reported values within most physical property databases. Furthermore, spinifex textures are occasionally logged as serpentine minerals rather than textural features that are replaced by amphiboles or chlorite (E.g. Eastern Gold Fields samples, notably KD8). This has posed a significant issue with regards to choosing actual serpentinised samples to study.

SWIR spectroscopy has been able to show relative changes of dominant amphibole and FeMg-rich chlorite mineral abundances in mafic rocks (Figures 9-12). Similarly, relative changes in talc-carbonate and Mg-rich chlorite mineral abundances have been shown in ultramafic rocks (Figures 13-15). Subsequently, bivariate physical property plots overlain with SWIR abundance data are investigated in further detail:

- Talc-Mg-rich chlorites have a magnetic susceptibility several orders of magnitude higher than mafic samples as well as a relatively low p-wave velocity (Figures 16-18);
- The bulk of carbonate minerals are principally talc, with calcite, ankerite, dolomite, and magnesite (Figures 19-21). An increase in apparent porosity and decrease in p-wave velocity is shown to occur with an increasing abundance of talc-carbonate minerals.
- An increase in density of mafic rocks is observed to correlate with an increase in amphibole content (Figures 22-25). This is in agreement with Bourne et al. (1993).

However, a population of serpentine mineral data is shown to increase in abundance with increasing in p-wave velocity and magnetic susceptibility, and decrease density and apparent porosity (Figures 26-27). The increase in p-wave velocity is at odds with most literature (Dentith & Mudge, 2014), yet the increase in magnetic susceptibility and decrease in density is in agreement (Toft et al., 1990). Quartz, pyroxene, olivine minerals, as well as serpentine mineral species are unable to be measured by SWIR spectroscopy. Only X-ray diffraction (XRD) is able to quantify and determine serpentine mineral species. Density values of 2.7-2.75 g/cm^3 suggest that olivine and pyroxene are not constituent minerals. It is more likely that this population has either undergone silicification and or is perhaps a different species of serpentine mineral, i.e. antigorite, as opposed to the more common lizardite (Christensen, 2004). Due to this uncertainty, SWIR classification should be treated with greater caution when attempting to classify physical property data of serpentinised rocks. As well, it is noted that greater uncertainty of SWIR mineral abundance values will occur where there is significant overlap between SWIR active minerals. The interpretation and classification of wavelength shifts for these minerals may be more appropriate than determination of abundance data in these circumstances.

CONCLUSIONS

SWIR spectroscopy is shown to be useful for the classification of ultramafic and mafic rocks. Furthermore, as chlorite, amphibole and carbonate group minerals are dominant within talc-carbonate alteration assemblages, SWIR spectroscopy is suitably able to quantify the degree of alteration. Lateral variations in spectral absorption features allow the sub-classification of chlorite, carbonate, and amphibole mineral species via magnesium and iron content. These data are also useful for the interpretation of physical property data.

Serpentine minerals are readily identifiable within the SWIR. However, the identification of mineral species, i.e. lizardite, antigorite, chrysotile, is needed so as to better constrain physical property data. Quartz, olivine and pyroxene may also be dominant constituents in serpentinised rocks. These minerals are unable to be measured within the SWIR. As such, care must be exercised when interpreting a potentially misleading SWIR normalised mineral abundance of serpentine. Care must also be exercised when interpreting SWIR mineral abundance data, particularly where 3 or more SWIR active minerals may present. Overlapping wavelength features may complicate the reliability of the spectral unmixing identification processes.

ACKNOWLEDGMENTS

This study is a part of an ongoing PhD research project at UWA, and is funded by a MRIWA postgraduate research scholarship and an ASEG research foundation grant. An ASD Inc. Students in Mining Program grant has generously provided the use of TerraSpec 4 instrumentation and support. Financial and data support for this project is kindly provided by Northern Star Resources. The Department of Mines & Petroleum Kalgoorlie Core Library team are thanked for lending drill core specimens, and assistance with numerous viewings. The authors wish to thank Dr. Sue Murray and the Plutonic Gold Mine exploration team for their ongoing support, hospitality and shared enthusiasm. Dr. Phil Schmidt (MagneticEarth), Assoc. Prof. Marco Fiorentini (UWA), Alejandro Anchundia (Terraplus), and Mr. Peter McMullen (GeoResults Pty Ltd.) are acknowledged for insightful discussions.

REFERENCES

Adams, C. & Dentith, M., 2016, Towards an understanding of the effects of alteration on the physical properties of mafic and ultramafic rocks: ASEG-PESA Conference, Adelaide, Australia, Extended Abstract.

Adams, C. & Dentith, M., 2017, Magnetic Measurements on Diamond Drill-Core: Are We Really Measuring Magnetic Susceptibility?: Exploration'17 Conference, Toronto, Canada, Extended Abstract.

Adams, C. & Dentith, M., 2018, Practical Considerations & Good Protocol for the Interpretation of Ultramafic & Mafic Rock Physical Property Data: AEGC2018, Sydney, Australia, Extended Abstract.

Bourne, B.T., Trench, A., Dentith, M., & Ridley, J.R., 1993, Physical property variations within Archaean granite-greenstone terrane in the Yilgarn Craton, Western Australia: Exploration Geophysics, 24, 367-374.

Chistensen, N. I., 2004, Serpentinites, Peridotites, and Seismology: International Geology Review, 46 (9), 795-816.

Clark, D.A., 2014, Methods for determining remanent and total magnetisations of magnetic sources – a review: Exploration Geophysics, 45, 271-304.

Dentith, M., Adams, C., & Bourne, B.T., 2017, Petrophysics and Exploration Targeting: Best Practice and Applications: Target2017 Conference, University of Western Australia, Perth, Australia.

Dentith, M., & Mudge, S.T., 2014, Geophysics for the Mineral Exploration Geoscientist: Cambridge Univeristy Press, United Kingdom, pp438.

Emerson, D.W., 1990, Notes on Mass Properties of Rocks – Density, Porosity, Permeability: Exploration Geophysics, 21, 209-216.

Hauff, P., 1983, An overview of VIS-NIR-SWIR field spectroscopy as applied to precious metals exploration: Spectral International Inc., Arvada, Colorado, USA, pp71.

Henkel, H., 1994, Standard diagrams of magnetic properties and density – a tool for understanding magnetic petrology: Journal of Applied Geophysics, 32, 43-53.

Lipton, I.T., & Horton, J.A., 2014, Measurement of bulk density for resource estimation – methods, guidelines and quality control: Mineral Resource and Ore Estimation – The AusIMM Guide to Good Practice, 2nd edition, Monograph 30, 97-108.

MagneticEarth, 2015, The QMeter Instruction Manual: MagneticEarth Pty Ltd., pp16.

Toft, P.B., Arkani-Hamed, J., & Haggerty, S.E., 1990, The effects of serpentinization on density and magnetic susceptibility: a petrophysical model: Physics of Earth and Planetary Interiors, 65, 137-157.

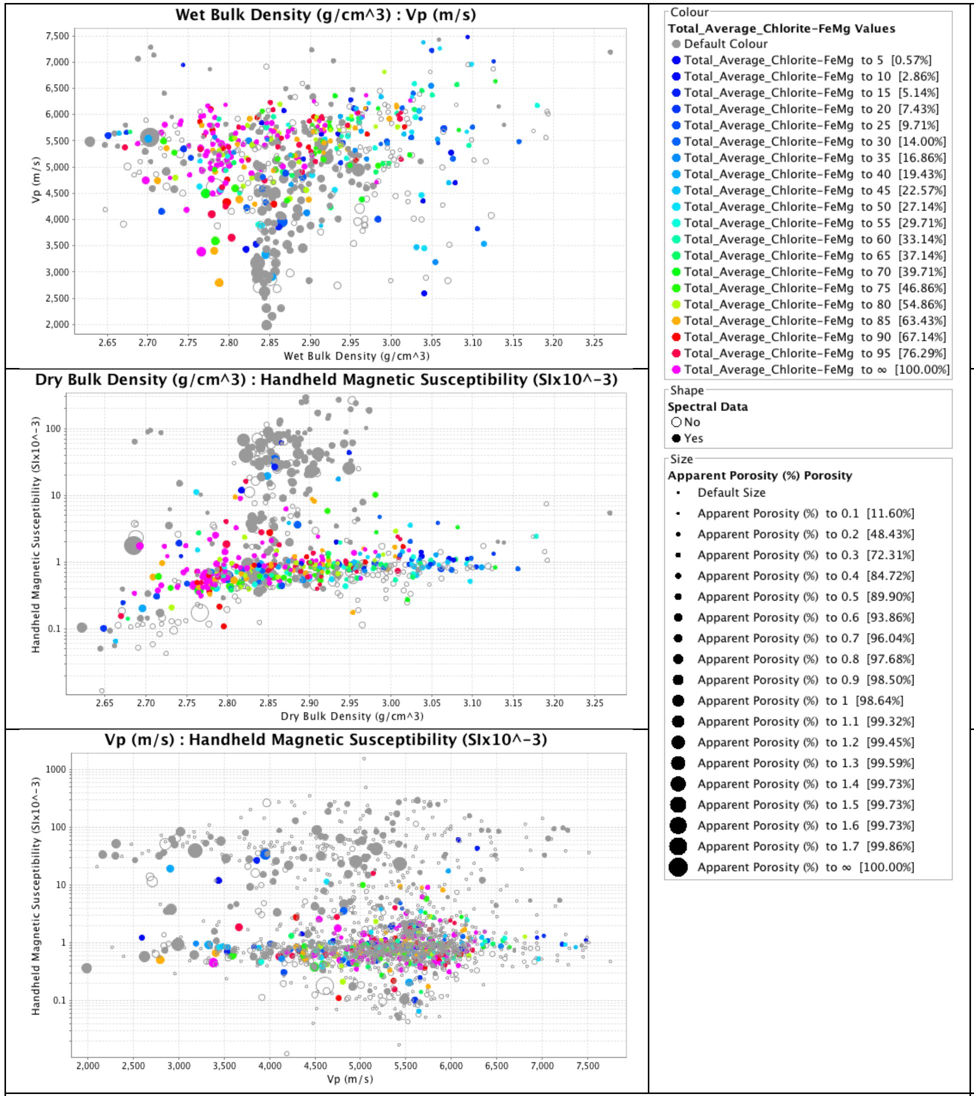

Figures 9-12: P-wave velocity vs wet bulk density, i.e. acoustic impedance (top); magnetic susceptibility vs dry bulk density (middle), i.e. mass susceptibility; and magnetic susceptibility vs p-wave veolcity (bottom). Data points are coloured by abundance (%) of **FeMg-Chlorite** minerals normalised to minerals measured within SWIR spectrum. Grey data points show measured physical properties that have no spectral data. Points are sized by **apparent porosity (%).** Axes of magnetic susceptibility are in log-scale.

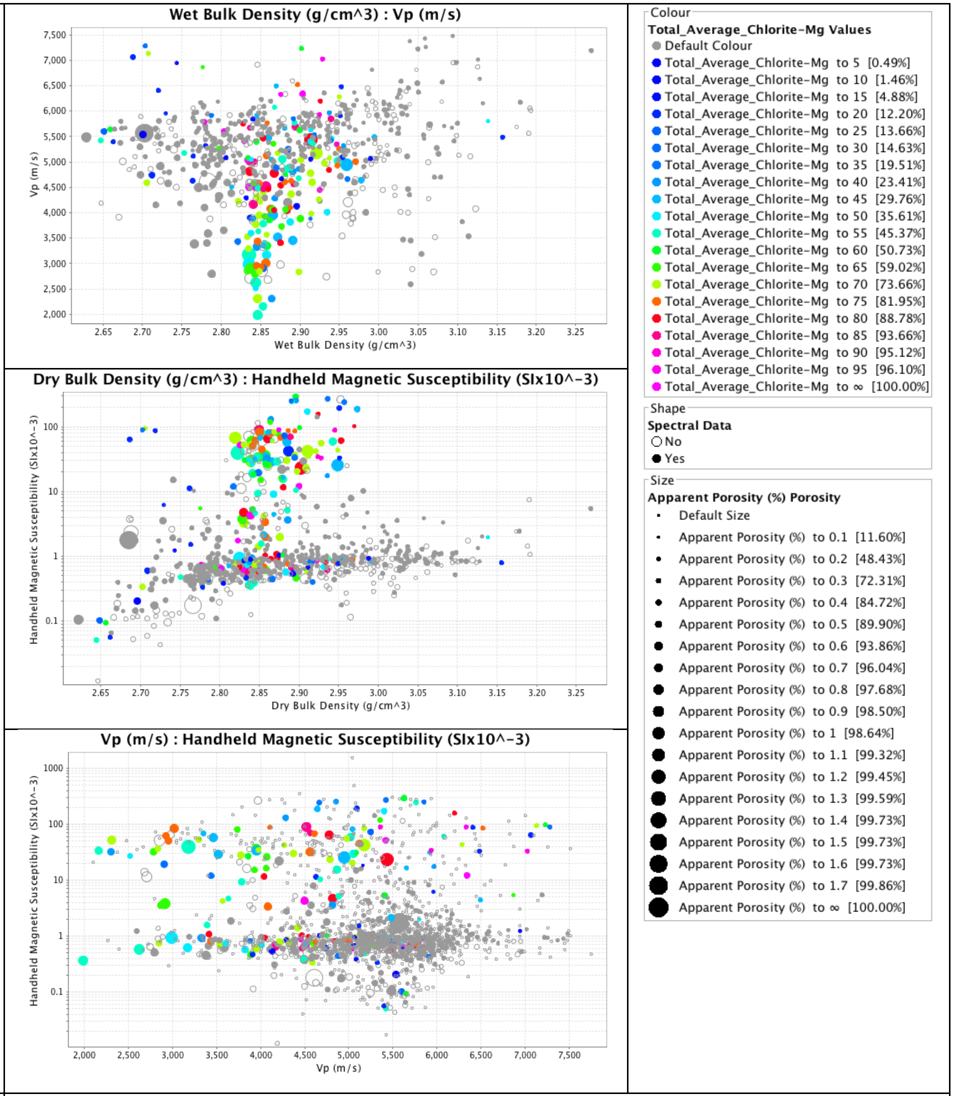

Figures 13-15: P-wave velocity vs wet bulk density, i.e. acoustic impedance (top); magnetic susceptibility vs dry bulk density (middle), i.e. mass susceptibility; and magnetic susceptibility vs p-wave veolcity (bottom). Data points are coloured by abundance (%) of **Mg-Chlorite** minerals normalised to minerals measured within SWIR spectrum. Grey data points show measured physical properties that have no spectral data. Points are sized by **apparent porosity (%).** Axes of magnetic susceptibility are in log-scale.

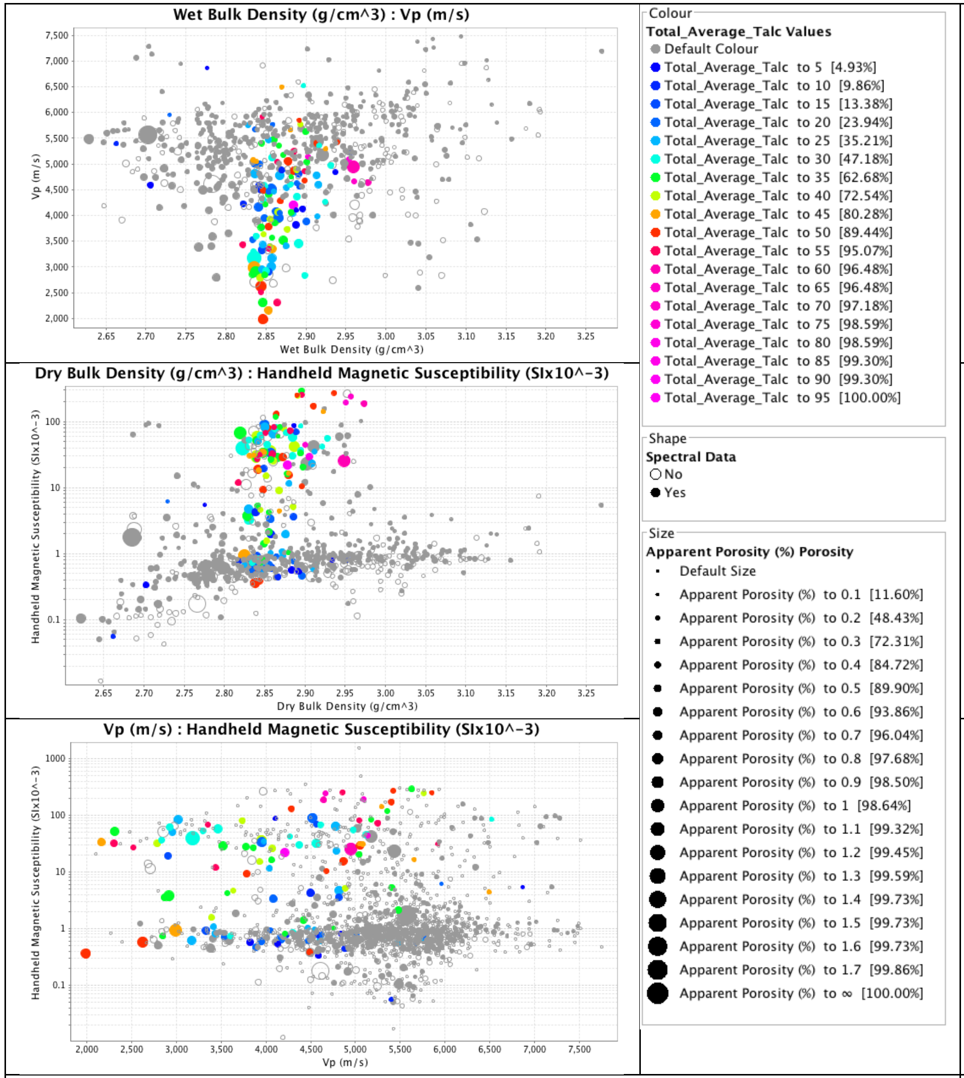

Figures 16-18: P-wave velocity vs wet bulk density, i.e. acoustic impedance (top); magnetic susceptibility vs dry bulk density (middle), i.e. mass susceptibility; and magnetic susceptibility vs p-wave veolcity (bottom). Data points are coloured by abundance (%) of **Talc** normalised to minerals measured within SWIR spectrum. Grey data points show measured physical properties that have no spectral data. Points are sized by **apparent porosity (%).** Axes of magnetic susceptibility are in log-scale.

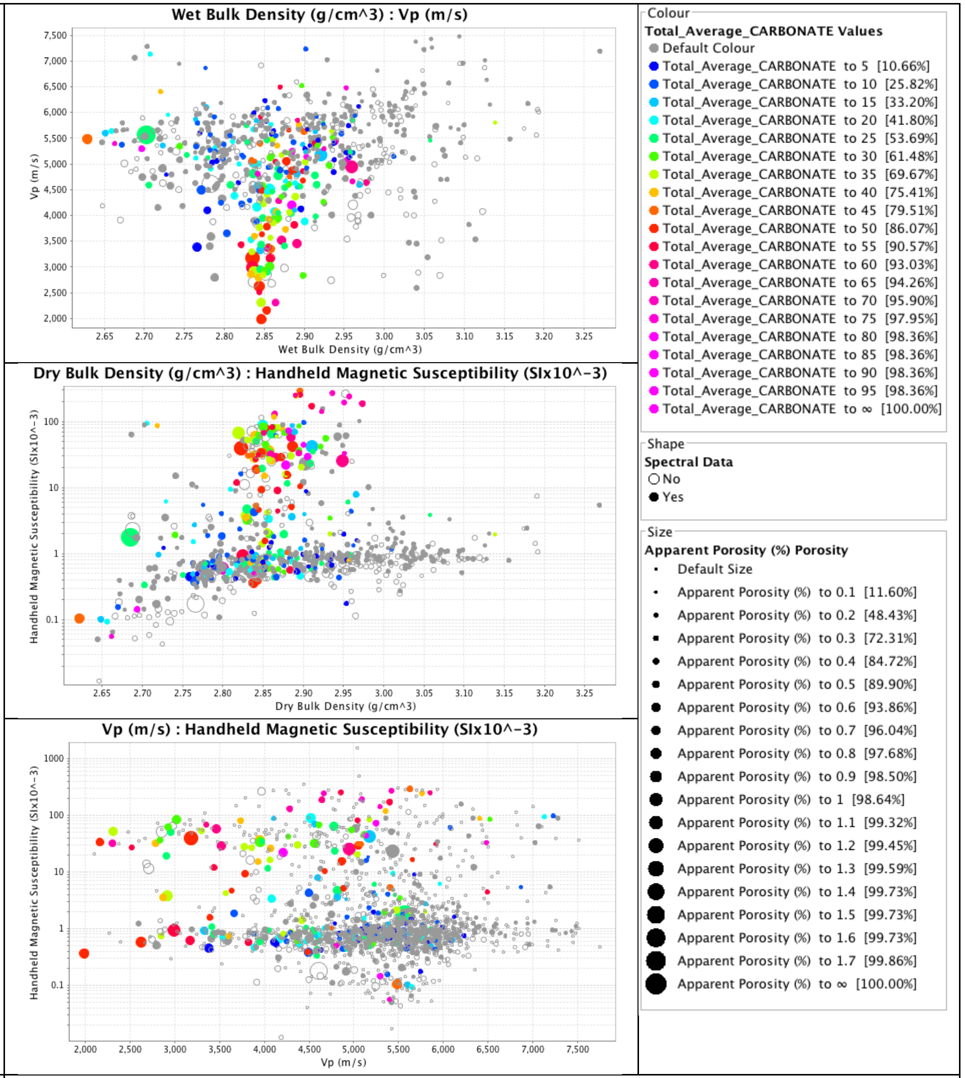

Figures 19-21: P-wave velocity vs wet bulk density, i.e. acoustic impedance (top); magnetic susceptibility vs dry bulk density (middle), i.e. mass susceptibility; and magnetic susceptibility vs p-wave veolcity (bottom). Data points are coloured by abundance (%) of **carbonate** minerals normalised to minerals measured within SWIR spectrum. Grey data points show measured physical properties that have no spectral data. Points are sized by **apparent porosity (%).** Axes of magnetic susceptibility are in log-scale.

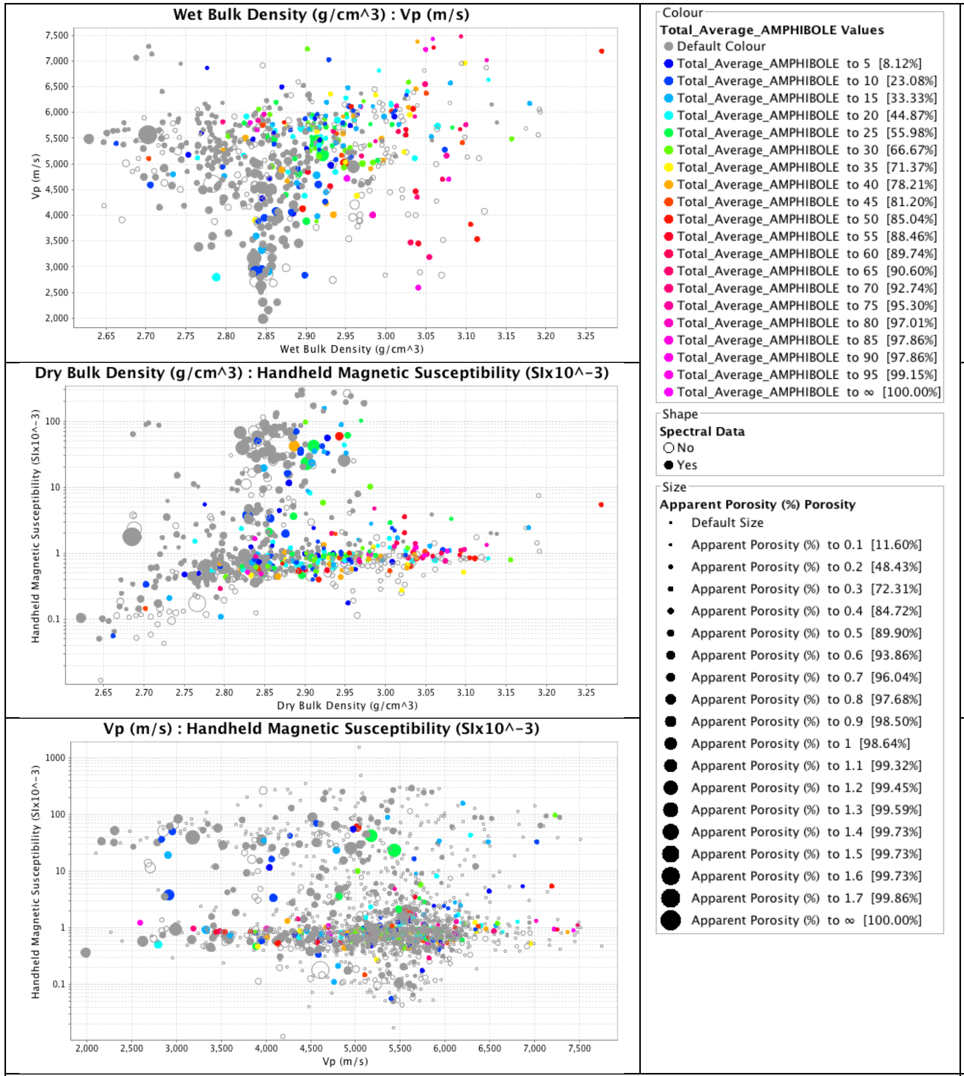

Figures 22-25: P-wave velocity vs wet bulk density, i.e. acoustic impedance (top); magnetic susceptibility vs dry bulk density (middle), i.e. mass susceptibility; and magnetic susceptibility vs p-wave veolcity (bottom). Data points are coloured by abundance (%) of **amphibole** minerals normalised to minerals measured within SWIR spectrum. Grey data points show measured physical properties that have no spectral data. Points are sized by **apparent porosity (%).** Axes of magnetic susceptibility are in log-scale.

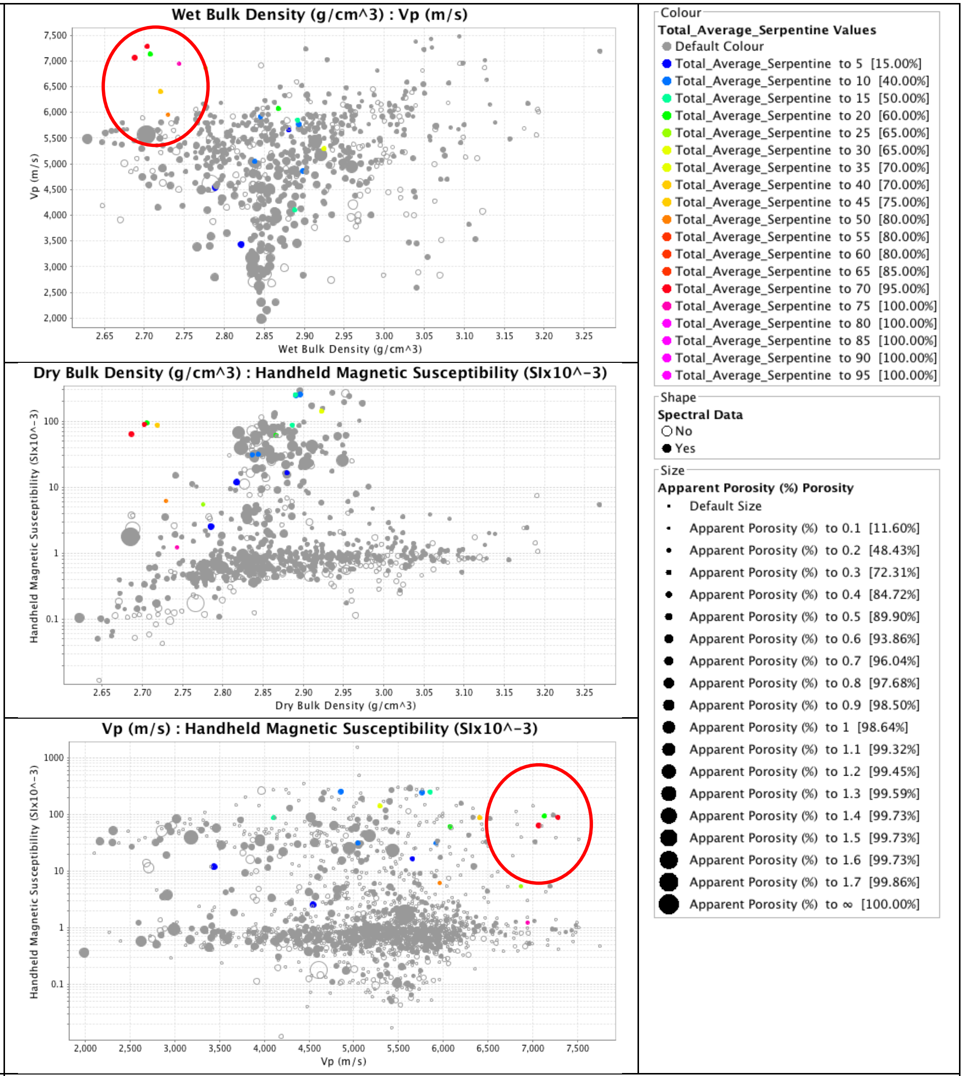

Figures 26-27: P-wave velocity vs wet bulk density, i.e. acoustic impedance (top); magnetic susceptibility vs dry bulk density (middle), i.e. mass susceptibility; and magnetic susceptibility vs p-wave veolcity (bottom). Data points are coloured by abundance (%) of **serpentine** minerals normalised to minerals measured within SWIR spectrum. Grey data points show measured physical properties that have no spectral data. Points are sized by **apparent porosity (%).** Axes of magnetic susceptibility are in log-scale. Red ellipses show anomalous, i.e. high Vp, serpentine mineral data.